Received: 30 October 2023 | Revised: 11 January 2024 | Accepted: 17 January 2024

DOI: 10.1002/biot.202300587

Biotechnology Journal

RESEARCH ARTICLE

The choice of ultra-low attachment plates impacts primary human and primary canine hepatocyte spheroid formation, phenotypes, and function

Chen Xing[1] | Aurino Kemas[1] | Evgeniya Mickols[2] | Kathrin Klein[3,4] | Per Artursson[2] | Volker M. Lauschke[1,3,4]

[1]Department of Physiology and Pharmacology, Karolinska Institute, Stockholm, Sweden

[2]Department of Pharmacy, Uppsala University, Uppsala, Sweden

[3]Dr Margarete Fischer-Bosch Institute of Clinical Pharmacology, Stuttgart, Germany

[4]University of Tübingen, Tübingen, Germany

Correspondence
Volker M. Lauschke, Department of Physiology and Pharmacology, Karolinska Institutet, SE-171 77 Stockholm, Sweden.
Email: volker.lauschke@ki.se

Funding information
Swedish Research Council, Grant/Award Numbers: 2019-01837, 2021-02801; Ruth och Richard Julins Stiftelse, Grant/Award Number: 2021-00158

Abstract

Organotypic three-dimensional liver spheroid cultures in which hepatic cells retain their molecular phenotype and functionality have emerged as powerful tools for preclinical drug development. In recent years a multitude of culture systems have been developed; however, a thorough side-by-side benchmarking of the different methods is lacking. Here, we compared the performance of ten different 96- and 384-well microplate types to support spheroid formation and long-term culture. Specifically, we evaluated differences in spheroid formation kinetics, viability, functionality, expression patterns, and their utility for hepatotoxicity assessments using primary human hepatocytes (PHH) and primary canine hepatocytes (PCH). All 96-well plates enabled formation of PHH liver spheroids, albeit with differences between plates in spheroid size, geometry, and reproducibility. Performance of different 384-wells was less consistent. Only 6/10 microplates supported the formation of PCH aggregates. Interestingly, even if PCH aggregates in these six microplates were more loosely packed than PHH spheroids, they maintained their function and were compatible with long-term pharmacological and toxicological assays. Overall, Corning and Biofloat plates showed the best performance in the formation of both human and canine liver spheroids with highest viability, most physiologically relevant phenotypes, superior CYP activity and lowest coefficient of variation in toxicity assays. The presented data constitutes a valuable resource that demonstrates the impacts of current ultra-low attachment plates on liver spheroid metrics and can guide evidence-based plate selection. Combined, these results have important implications for the cross-comparison of different studies and can facilitate the standardization and reproducibility of three-dimensional liver culture experiments.

Abbreviations: ANOVA, analysis of variance; APAP, acetaminophen; BSEP, bile salt export pump; C_{max}, peak serum concentration; CPZ, chlorpromazine; CV, coefficient of variation; CYP, cytochrome P450; DMSO, dimethyl sulfoxide; ECM, extracellular matrix; FBS, fetal bovine serum; LC/MS-MS, liquid chromatography tandem mass spectrometry; NAM, new approach methodology; NAPQI, n-acetyl-p-benzoquinonimine; PCA, principal component analysis; PCH, primary canine hepatocytes; PHH, primary human hepatocytes; SEM, standard error of the mean; TRO, troglitazone; ULA, ultra-low attachment.

KEYWORDS
cell culture, liver spheroids, medical biotechnology, metabolism, 3D cell culture

1 | INTRODUCTION

The discovery of safe and effective medicines relies on the accurate clinical translation of findings based on preclinical models. The liver is among the organ systems most commonly affected by adverse drug reactions, and hepatotoxicity is a main reason for the attrition of drug candidates and the withdrawal of drugs from the market.[1] Additionally, the liver is a key determinant of the pharmacokinetics of newly developed compounds and accurate prediction of formed metabolites, drug bioavailability, and clearance constitute integral steps in preclinical drug development. Animal tests have long been an essential part of the preclinical testing pipeline with an estimated 190 million animals used in medical research globally per year [2]. Regulatory guidelines require safety and tolerability data from at least one rodent and one non-rodent species, before first-in-man trials. Of these, Beagle dogs are the most popular for preclinical safety testing and pharmacokinetic studies.[3] However, it is becoming increasingly clear that animals are overall poor predictors of human drug efficacy and safety [4–6]. This awareness has resulted in the increased adoption of new approach methodologies (NAMs) in preclinical pharmacology and toxicology [7]. These developments are further supported by recent changes in legislation that end the blanket mandate for animal testing [8].

To facilitate early prediction of hepatotoxicity and pharmacokinetic properties, organotypic culture models of primary hepatocytes have emerged as versatile in vitro models [9–12]. Specifically, three-dimensional liver spheroids are increasingly utilized as they allow for the maintenance of physiologically relevant phenotypes and functions for multiple weeks [13–15]. Furthermore, liver spheroids have been well characterized as model systems for the prediction of toxicity [16,17] and clearance [18–20] where they outperform previous culture systems, such as sandwich or suspension cultures. Multiple different methodologies for liver spheroid culture have been described. Spheroid formation techniques include hanging drops, agitation-based methods, as well as aggregation in ultra-low attachment (ULA) plates [21,22]. Particularly the latter enables the rapid, inexpensive and scalable formation of thousands of spheroids of well-defined sizes in 96- or 384-well plate formats. Once spheroids are formed, they can be maintained in different media with or without the addition of serum. For media compositions, extensive careful benchmarking studies have contributed to protocol standardization and have facilitated cross-study reproducibility and comparability [23]. However, similar studies have not been conducted to compare different culture plates despite the wide range of available products on the market.

Different plates differ in geometry, which in turn can impact spheroid formation kinetics and alter evaporation [24]. Furthermore, different coatings can alter surface properties and biomechanical cues, which can influence viability, molecular phenotypes, and stability.[25–27] Surface treatments and materials can also affect the absorption of small molecules [28], thereby changing cellular exposure levels. To optimize spheroid cultures and improve cross-study and cross-center comparability, it is thus imperative to be aware of the differences caused by plate parameters.

To provide practical guidance for plate selection, we here compared the performance of ten different 96- and 384-well ULA microplates. We generated spheroids from primary human hepatocytes (PHH) and found considerable differences in spheroid formation kinetics, viability, functionality, gene expression profiles, and their utility in hepatotoxic assessments. To facilitate utility for translational research, we furthermore generated primary canine hepatocyte (PCH) spheroids and analyzed inter-species differences. These investigations provide a basis for evidence-based microplate selection for liver spheroid studies and aspire to promote standardization of ULA plate parameters.

2 | MATERIAL AND METHODS

2.1 | Spheroid culture

Cryopreserved PHH were obtained from patients undergoing liver resection at the Department of Surgery at Uppsala University Hospital, Sweden (Ethical Approval no. 2009/028, amended 2018/1108). PHH were isolated as previously described [29]. In brief, the liver tissue was rinsed using Hypothermosol FRS (Biolife Solutions), cannulated, and perfused with collagenase and protease buffers to release cells from the tissue matrix. For cryopreservation, the hepatocytes were resuspended in CryoStor CS10 solution (BioLife Solutions) supplemented with 10% fetal bovine serum (FBS) and stored at -150°C until use. Cryopreserved PCHs from male Beagle dogs were commercially acquired (BioIVT).

Spheroids were seeded and cultured as previously described [30]. Specifically, cells were thawed in a 37°C water bath. Subsequently, the cell suspension was transferred to thawing medium (Williams E medium containing 27% isotonic Percoll) and centrifuged at 100 × *g* for 10 min. The supernatant was aspirated, and hepatocytes were washed and resuspended in warm culture medium (Williams E medium with 2 mM L-glutamine, 100 units mL^{-1} penicillin, 100 μg mL^{-1} streptomycin, 10 μg mL^{-1} insulin, 5.5 μg mL^{-1} transferrin, 6.7 ng mL^{-1} sodium selenite, 100 nM dexamethasone) with 10% fetal bovine serum (FBS). After cell counting, PHH were then seeded into ten different models of 96- or 384-well ULA plates at a concentration of 1500 viable PHH or PCH per well (Table S1). In 96-well plates, cells were cultured in 100 μL while spheroids were cultured in 80 μL of medium in 384-well plates. When the spheroids were sufficiently compact, medium was exchanged to serum-free culture medium. Notably, both spheroid formation and maintenance occurs under scaffold-free conditions. Spheroid exposures were started 7 days (PHH) or 10 days (PCH)

after seeding. Spheroids were maintained for up to 3 weeks with a medium change every 48 to 72 h.

2.2 | Gene expression analysis

RNA was isolated from ≥30 pooled spheroids per sample using the Zymo Quick-RNA Microprep Kit (Zymo Research) and expression of selected genes was quantified using the Biomark HD system (Fluidigm) with a FLEXsix integrated fluidic circuit (IFC, Fluidigm). The utilized gene expression assays are provided in Table S2. The gene expression levels were calculated using the ΔΔCt method with two to three housekeeper genes as reference.

2.3 | Immunofluorescence

PHH spheroids were fixed overnight in 4% formaldehyde at 4°C, cryoprotected in 30% sucrose for 2 days at room temperature and then embedded in Tissue-Tek OCT compound (Sakura). Spheroid cryosections (8 µm) were stained for CYP3A4 (PAP011, 1:5000, Cypex) and albumin (sc51515, 1:200, Santa Cruz), and mounted in ProLong Gold antifade reagent with DAPI (ThermoFisher). Immunofluorescence images were acquired with an LSM 880 confocal microscope (Zeiss).

2.4 | Assessment of cell viability

Cell viability was assessed using the CellTiter-Glo Luminescent Cell Viability Assay (Promega) on a SpectraMax iD3 Multi-Mode Microplate Reader (Molecular Devices). Chlorpromazine hydrochloride (CPZ, Sigma) and troglitazone (TRO, Sigma) stock solutions were prepared in dimethyl sulfoxide (DMSO) while acetaminophen (APAP, Sigma) was dissolved in culture medium. Exposure values (C_{max}) were obtained from the published literature [16] as follows: APAP = 136 µM, CPZ = 0.84 µM, and TRO = 6.08 µM.

2.5 | Metabolic profiling

Single PHH spheroids were incubated for 4 h at 37°C with a cocktail of CYP substrates: 10 µM midazolam (CYP3A4), 5 µM dextromethorphan (CYP2D6), 10 µM amodiaquine (CYP2C8), and 10 µM diclofenac (CYP2C9), while CPH were incubated with 10 µM midazolam (CYP3A4) and 5 µM dextromethorphan (CYP2D6). The reactions were stopped by mixing with ice-cold acetonitrile/water (60:40); 10 nM warfarin was used as internal standard. The respective metabolites 1-hydroxymidazolam, dextrorphan, N-desethylamodiaquine and 4-hydroxy diclofenac were measured by liquid chromatography tandem mass spectrometry (LC/MS-MS). Samples were centrifuged for 10 min at 4°C with 3500 × *g*, and supernatants were analyzed on a Waters Acquity UPLC coupled to Waters Xevo TQ MS with electrospray ionization. Compounds were separated with a 2 min gradient elution of acetonitrile and 0.1% formic acid (flowrate 0.5 mL min^{-1}) on a Waters BEH C18 column, 2.1 × 50 mm (1.7µm) at 60°C. Peaks were quantified using MassLynx Software V4.2 with TargetLynx.

2.6 | Statistical analyses

Statistical analyses were performed with GraphPad Prism (Version 9.5.1). No outlier elimination was performed, and all obtained data points were included into the analyses. *p*-values < 0.05 were considered significant.

3 | RESULTS

3.1 | The choice of ULA microplates impacts PHH spheroid formation kinetics and morphology

To compare different microplates for liver spheroid formation, we first monitored the aggregation of PHH into spheroids. Over the course of 7 days, PHH aggregated and compacted into spheroids with diameters of 200 to 300 µm in almost all microplates (Figure 1A,B). The establishment of three-dimensional liver spheroids as a standardized methodology in preclinical pharmacology and toxicology requires high reproducibility. To this end, it is crucial that cells assemble into a single spheroid in each well without the formation of satellites. Across 96-well plates, the cell suspensions aggregated predominantly (> 90%) into one single spheroid (Figure 1C). In 384-well plates, aggregation was overall less uniform and only Biofloat384 well plates showed uniform formation of single spheroids. In contrast, in Greiner384 plates, cells formed multiple small spheroids with diameters ranging from 70 to 100 µm, suggesting that these plates are of limited use for high-throughput pharmacological or toxicological experiments.

During aggregation, spheroid diameters decreased over time with similar kinetics across 96-well plates (Figure 1D). Among the 384-well plates, spheroids formed considerably faster in the Biofloat384 plates with fully formed aggregates being visible after 3 days compared to 5 or 6 days in the other plate models (Figure 1E). Physical proximity may play an important role in the initial assembly of loose cell suspensions which depends on cell interaction through surface integrins [31]. The compact packing of PHHs after seeding facilitated by the specific geometry of the wells and the specific coating may thus account for the rapid organization of the cells into single spheroids in this plate model.

To compare plate performance in imaging-based high-throughput assays, we imaged entire plates with an automatic microscope on day 7 after seeding (Figure 1F). We did not observe systematic differences within plates between columns or rows. Also, no clear edge effect was observed. Overall, the morphology of spheroids agreed with the images captured by manual acquisition. Spheroids could not be automatically captured in PE384 plates since most spheroids were not located at the center of the wells, likely due to the flat-bottom design. The other plates were found to be compatible with automatic plate scans.

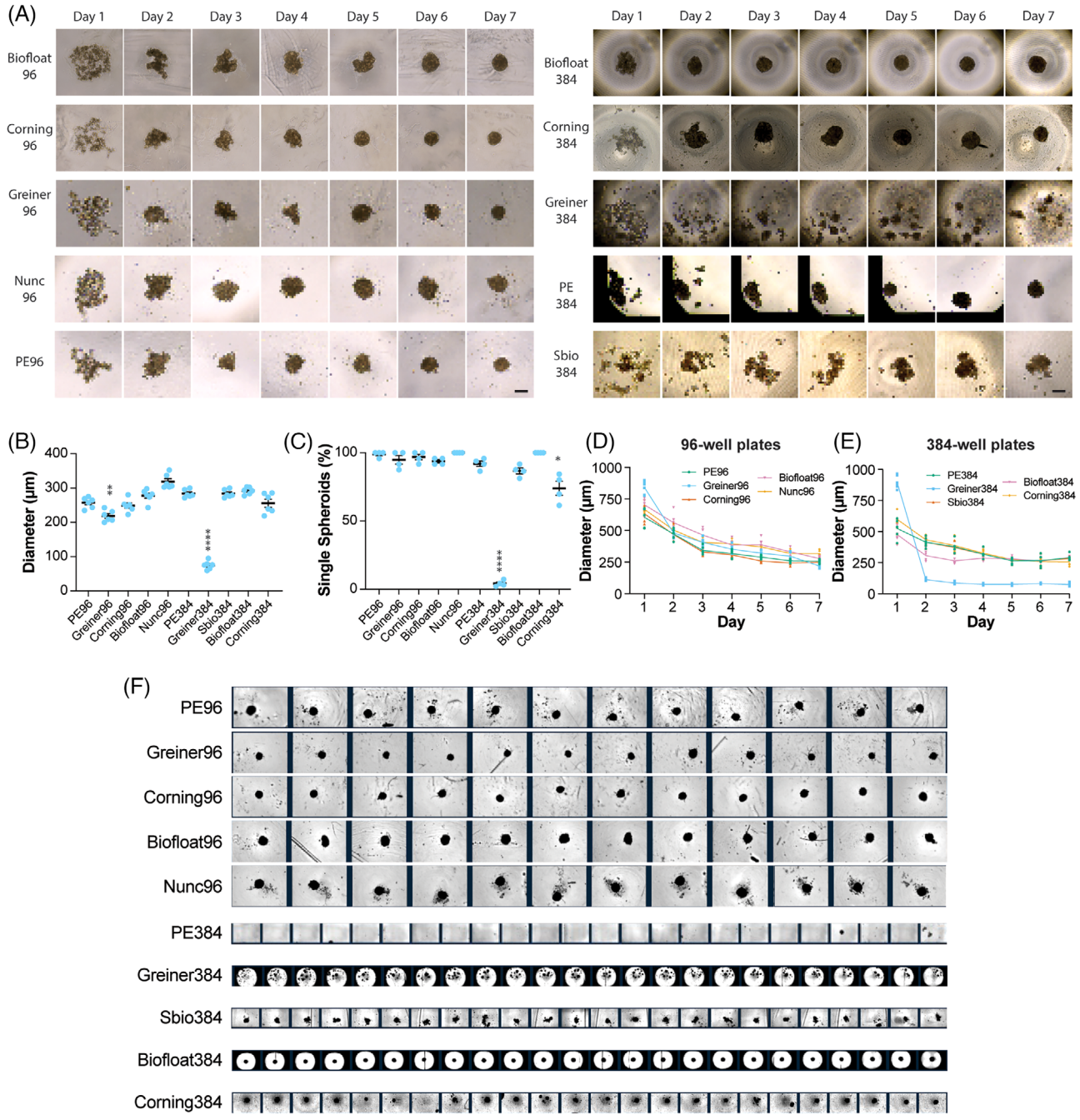

FIGURE 1 **Morphology and formation kinetics of human liver spheroids.** (**A**) Time series of brightfield images showing PHH spheroid formation. Scale bar = 200 µm. (**B**) Diameter of PHH spheroids on Day 7 after seeding in different types of plates. ** and **** indicate $p < 0.01$ and $p < 0.0001$ in an ANOVA test with Welch's correction. (**C**) The fraction of wells in which cells aggregated into one single spheroid. * and **** indicate $p < 0.05$ and $p < 0.0001$ in a Kruskal-Wallis test. Error bars indicate SEM. (**D-E**) Compaction kinetics of PHH over 7 days after seeding in 96-well plates (**D**) and 384-well plates (**E**). (**F**) High-throughput scan of spheroids in different types of plates. Only one representative row is shown per plate.

3.2 | Characterization of PHH spheroid phenotype, function, and stability in different ULA microplates

To assess the impact of the different microplates on long-term culture of PHH spheroids, we first assessed cell viability for up to 3 weeks (Figure 2A,B). In Corning96 and Corning384 plates, the initial ATP levels were maintained throughout the whole investigated period. In Biofloat384 and Biofloat96 plates, a significant drop in ATP levels could be observed at day 21 ($p < 0.01$). In all other plate models, ATP content dropped significantly already after 14 days. In Greiner96, PE96 and SBio384 plates, spheroid viability even dropped to levels < 25%, suggesting that these plates might be of limited use for

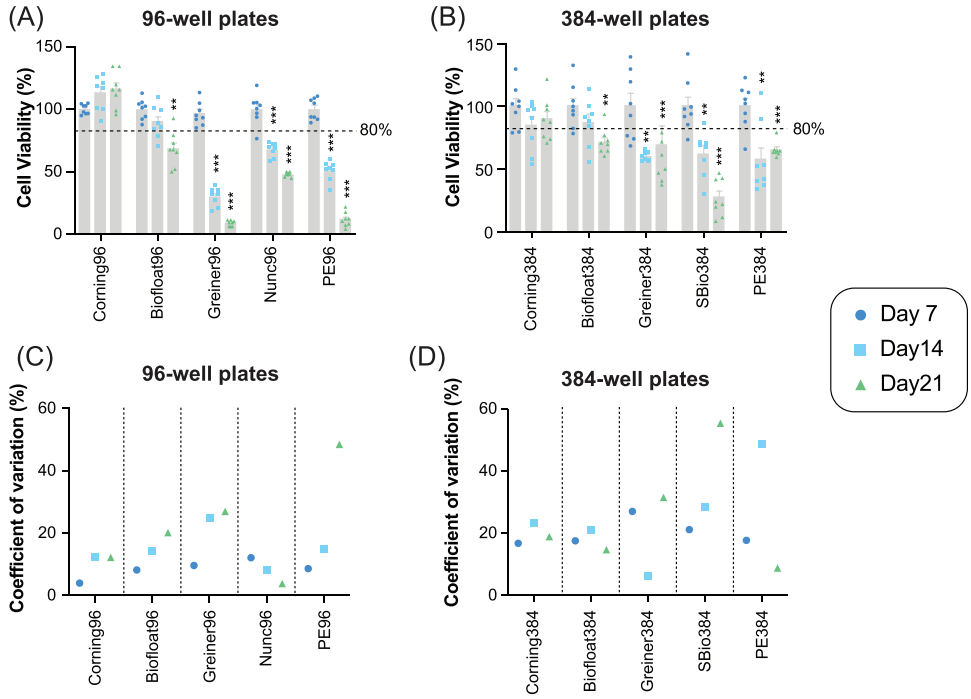

FIGURE 2 **Cell viability of human liver spheroids during 3 weeks of culture**. (**A**-**B**) Viability is shown for PHH spheroids after 7 days, 14 days, and 21 days of culture in 96-well plates (**A**) and 384-well plates (**B**). $n = 8$ per plate and time point. *, **, and *** corresponds to $p < 0.05$, $p < 0.01$, and $p < 0.001$ in a one-way ANOVA, respectively. Error bars indicate SEM. The dotted lines indicate 80% cell viability. (**C**-**D**) The coefficient of variation is shown for the different replicates after 7 days, 14 days, and 21 days of culture in 96-well plates (**C**) and 384-well plates (**D**).

long-term liver spheroid experiments. The variability between individual spheroids increased with culture time and was in general lower in 96-well plates compared to 384-well plates (Figure 2C,D). Most plates allowed reproducible measurements of cell viability (coefficient of variation [CV] < 20%) except for Greiner, PE and SBio plates in which CVs exceeded 30%.

Maintenance of phenotype and functionality of liver spheroids is critical for translational applications. We thus evaluated the expression of hepatic genes related to drug metabolism, ethanol catabolism, bile acid synthesis, and differentiation. Overall, drastic gene- and plate-specific differences were observed (Figure 3A; Figure S1). Expression of the differentiation markers *HNF1A*, *HNF4A*, and *ABCC2* did not markedly differ between microplates. *ALB*, *CYP2E1*, and *ABCC2* showed only marginal inter-plate variability, whereas the key drug metabolizing enzymes *CYP2D6* and *CYP3A4*, the bile acid genes *CYP7A1* and *ABCB11*, as well as the aldehyde dehydrogenase *ADH1A* exhibited pronounced differences. For the best performing plates (Corning96, Corning384, Biofloat96, and Biofloat384), we moreover supplemented these results at RNA level by immunofluorescence stainings. Notably, we found that the hepatic markers CYP3A4 and albumin remained expressed at protein level throughout the spheroids without apparent differences between these plate types (Figure S2).

Particularly, spheroid culture in Nunc96 plates resulted in major transcriptional alterations after 7 days and, while these differences equilibrated for *CYP2D6* and *CYP3A4* at later timepoints, expression of *CYP7A1* and *ABCB11* remained significantly different after 14 days. In agreement with these observations, the expression signature of spheroids cultured in Nunc96 plates formed a unique cluster after PCA at 7 days (Figure 3B). After 14 days however, two distinct clusters emerged, which separated transcriptional patterns in PE96, Nunc96, PE384, and Sbio384 from the other microplate types.

We complemented our expression analyses with measurements of metabolic activity. To this end, we incubated PHH spheroids after 7 days of culture with a cocktail of probe substrates for the metabolic enzymes (CYP1A2, CYP2C8, CYP2C9, and CYP3A4) and quantified the formed metabolites by LC-MS (Figure 3C). Striking differences between CYP activities were observed between microplates. PE96, Nunc96, PE384, and Sbio384 exhibited the lowest metabolic activities for all substrates, with CYP2C9 and CYP3A4 activity being below detection limit. In contrast, Biofloat384 and Corning384 showed the highest activities, closely trailed by Greiner96, Corning96, and Biofloat96. Among these plates, Biofloat96 and Biofloat384 plates showed the lowest variability between the different measurements. These results indicate that the choice of microplate constitutes an important parameter that can have pronounced impacts on results and interpretation of PHH spheroid studies.

3.3 | Microplates affect the outcomes of hepatotoxicity assessments in PHH spheroids

To test the impact of microplates on preclinical toxicity assays, PHH spheroids were exposed to hepatotoxins with different modes of

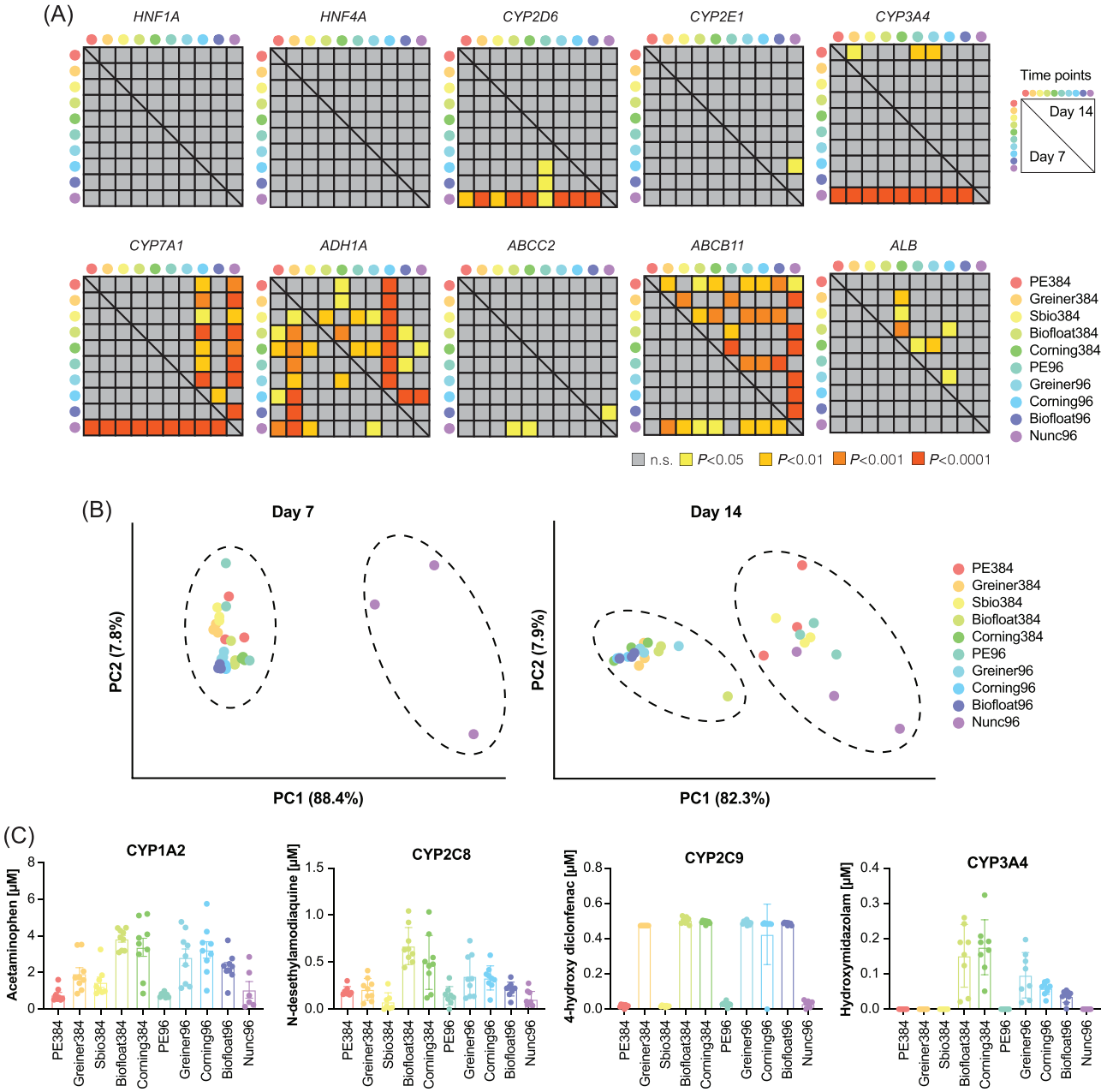

FIGURE 3 **The choice of culture plate affects molecular phenotypes and functions of human liver spheroids.** (**A**) Matrix representation of expression differences across ten important hepatic genes. The bottom left quadrant and top right quadrants indicate differences after 7 days and 14 days, respectively. $n = 3$ per plate and time point. Grey cells indicate $p \geq 0.05$ while yellow, light orange, dark orange, and red indicate $p < 0.05$, $p < 0.01$, $p < 0.001$, and $p < 0.0001$ in a one-way ANOVA, respectively. (**B**) Principal component analysis (PCA) can cluster microplate types based on transcriptional differences. Note that the differences along principal component 1 (PC1) that distinguish plate types are much larger than across principal component 2 (PC2), which separate replicates. (**C**) Column plots showing the levels of acetaminophen, N-desethylamodiaquine, 4-hydroxy diclofenac, and hydroxymidazolam, which serve measurements of the metabolic activities of CYP1A2, CYP2C8, CYP2C9, and CYP3A4.

action. Specifically, we selected APAP, TRO, and CPZ as prototypic compounds that exert toxicity via reactive metabolites, mitochondrial injury and cholestatic mechanisms, respectively. We evaluated toxicity both after a single dose (48 h exposure) and after 7 days of repeated exposures (Figure 4).

As expected, spheroid sensitivity increased with prolonged exposure for all compounds and plate types (Figure 4). Furthermore, we observed clear concentration-dependency of toxicity. This was most evident for TRO and CPZ whose higher concentrations caused complete cell death. The largest variability between plates was observed for intermediate TRO concentrations (5x c_{max}) where no toxicity was observed in Nunc96 and Sbio384 (viability > 80%) whereas isogenic liver spheroids in Corning96 and Corning384 were completely dead. Overall, the highest concentration of TRO and CPZ was required to detect in vitro toxicity in Nunc96 plates, whereas PHH spheroids in Corning384 and Biofloat384 were most sensitive with toxicity being

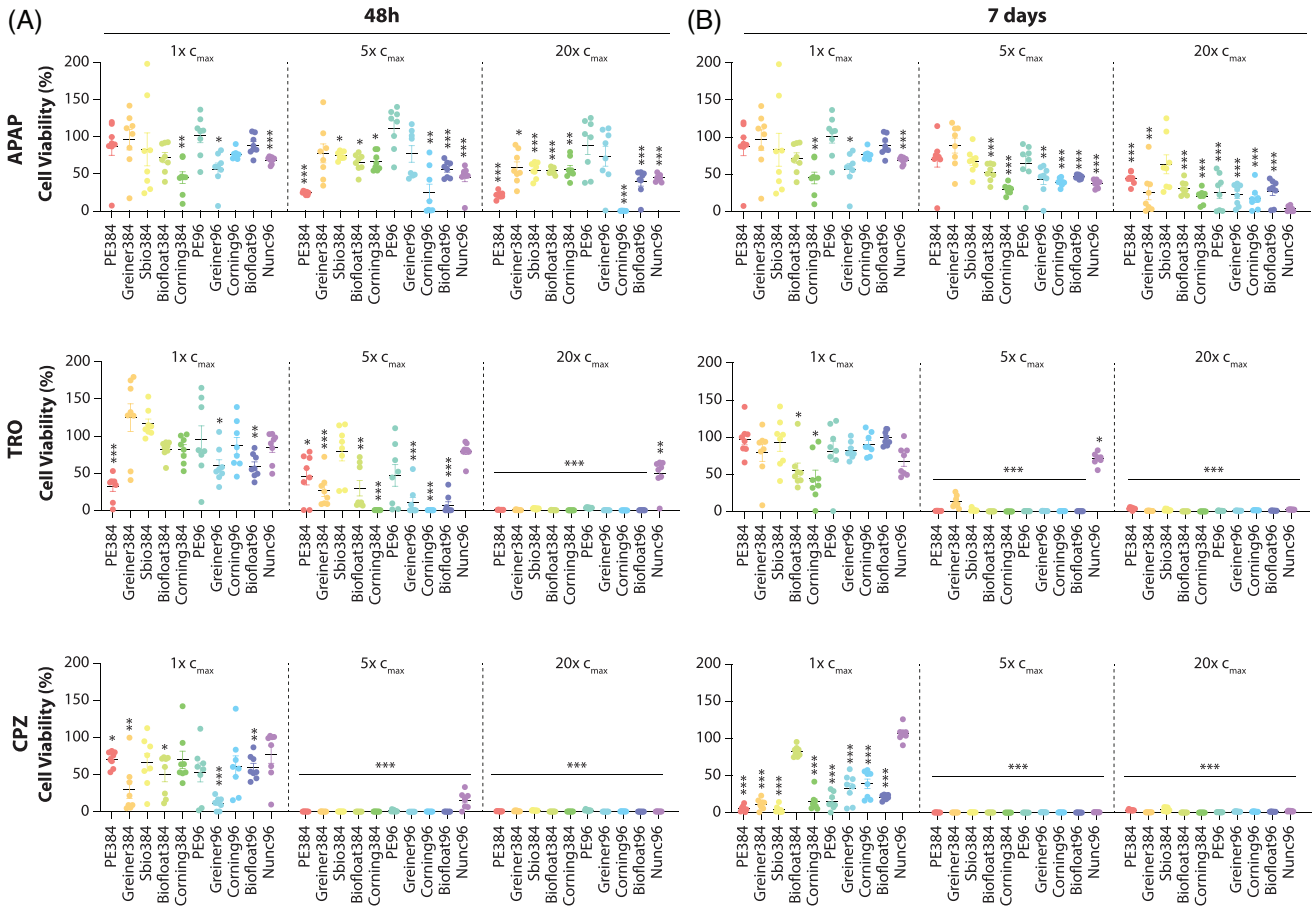

FIGURE 4 **Toxicity of prototypic hepatotoxins in human liver spheroids.** Cell viability was measured after a 48 h single exposure (**A**) and 7 days repeated exposures (**B**) for acetaminophen (APAP), troglitazone (TRO), and chlorpromazine (CPZ). $n = 8$ per plate, drug, and time point. Error bars indicate SEM. *, **, and *** correspond to $p < 0.05$, $p < 0.01$, and $p < 0.001$ in one-sample *t*-tests, respectively.

clearly evident even at the lowest concentration tested after 7 days exposure.

3.4 | Only few plate models support the formation of primary canine hepatocyte spheroids

Advanced organotypic cultures of primary hepatocytes of mouse, rat, minipig and cynomolgus monkey have been established to guide the selection of preclinical model species [16,32–34]. However, despite the popularity of Beagle dogs for preclinical drug safety testing, similar cultures have not been established for primary canine hepatocytes (PCH). We thus tested the potential of the different ULA plates to support PCH spheroid culture. In Corning96, PE96, Corning384, Sbio384, Biofloat96, and Biofloat384 microplates, PCH formed aggregates that were stable enough to be manipulated and transferred for endpoint measurements. In contrast, in Greiner96, Nunc96, Greiner384, and PE384 microplates, PCH did not form stable aggregates and these plates were thus excluded from further analyses.

Spheroids generated in Corning96, PE96, and Corning384 maintained relatively high ATP levels for 17 days with the latter showing the highest ATP levels after 24 days of culture (Figure 5A). By comparison, ATP levels dropped more rapidly in Biofloat96, Biofloat384, and Sbio384. To further characterize the molecular phenotype of PCH aggregates, we evaluated the expression levels of the canine orthologues of eight hepatocyte-specific genes (Figure 5B). Specifically, we selected the canine transporter genes *ABCB11* and *ABCC2*, canine albumin (*ALB*) and transferrin (*TF*) as secretory markers, the hepatocyte master regulator *HNF4A* and the cytochrome P450s *CYP1A2*, *CYP2D15* (orthologue of human *CYP2D6*), and *CYP3A12* (orthologue of human *CYP3A4*). Upon aggregation (day 10), expression signatures in Sbio384 plates were different from the other plates, particularly due to altered expression of *ALB* and *CYP1A2*. However, unlike in PHH spheroids, differences between plates were comparable in magnitude to differences between replicates (Figure 5C; 10 days). In contrast, after extended culture (day 17), Corning384 plates showed differential expression of *ABCB11*, *ABCC2*, *ALB*, *CYP1A2*, *CYP2D15*, *CYP3A12*, and *TF* compared to the other microplates (Figure 5C; 17 days). At the phenotypic level, Corning96 and Biofloat96 exhibited the highest levels of metabolic activity, whereas activities in Sbio384, Corning384, and Biofloat384 were around two-fold lower (Figure 5D).

To evaluate hepatotoxicity in the different microplates, we exposed PCH aggregates to different concentrations of APAP, TRO, and CPZ (Figure 5E,F). After exposure to APAP, PCH aggregates generally main-

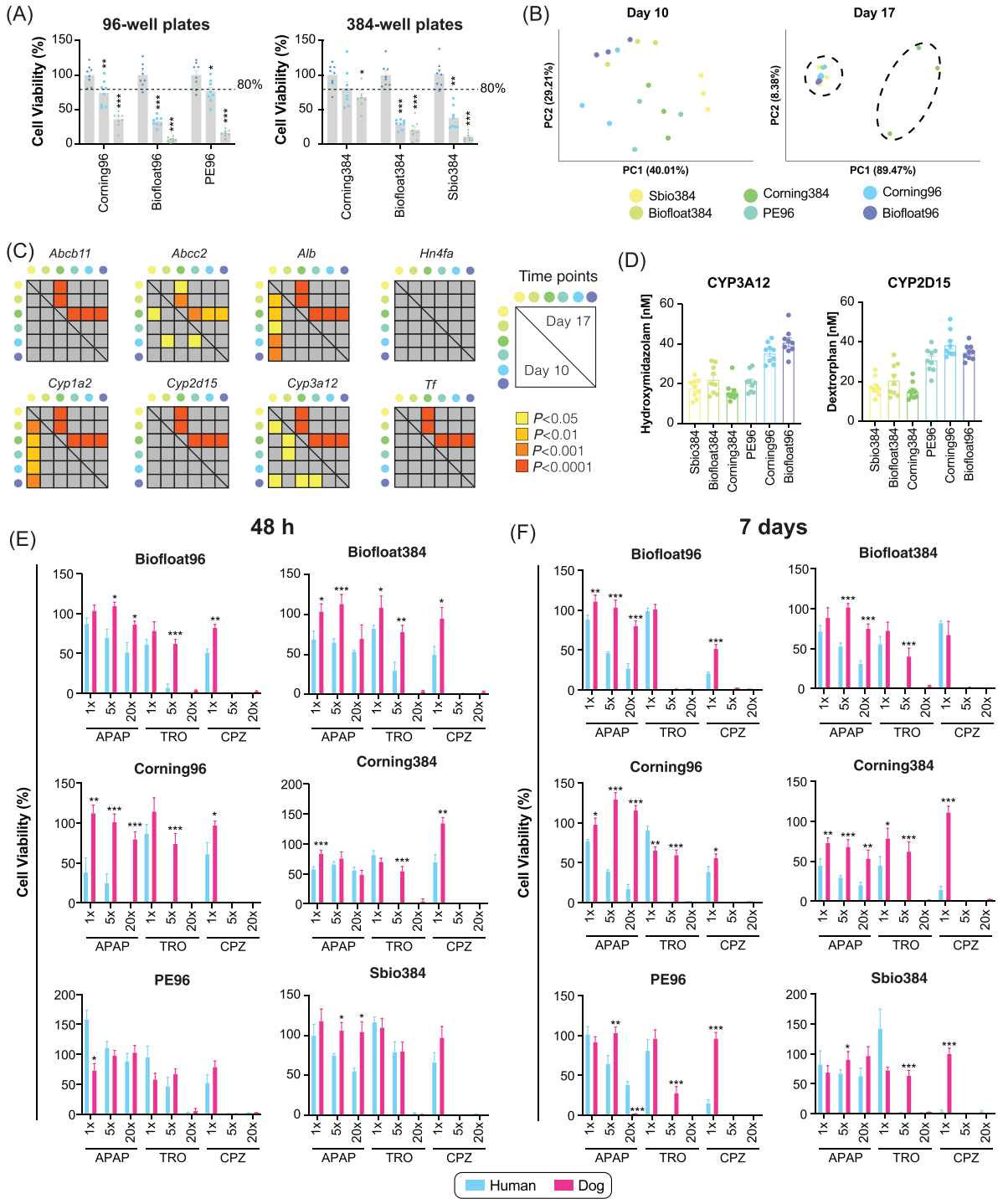

FIGURE 5 **Establishment and characterization of primary dog liver spheroids.** (**A**) Viability for PCH aggregates is shown after 10 days, 17 days, and 24 days of culture in 96-well plates and 384-well plates. Results are only shown for the six plate types that supported the formation of PCH aggregates. $n = 8$ per plate and time point. *, **, and *** corresponds to $p < 0.05$, $p < 0.01$, and $p < 0.001$ in a one-way ANOVA, respectively. Error bars indicate SEM. The dotted lines indicate 80% cell viability. (**B**) Matrix representation of expression differences across eight important hepatic genes. The bottom left and top right quadrants indicate differences after 10 days and 17 days, respectively. $n = 3$ per plate and time point. Grey cells indicate $p \geq 0.05$ while yellow, light orange, dark orange, and red indicate $p < 0.05$, $p < 0.01$, $p < 0.001$, and $p < 0.0001$ in a one-way ANOVA, respectively. (**C**) Principal component analysis (PCA) of expression patterns of the eight analyzed hepatic genes. (**D**) Column plots showing the levels of hydroxymidazolam and dextrorphan, which serve measurements of the metabolic activities of canine CYP3A12 (orthologue of human CYP3A4) and CYP2D15 (orthologue of human CYP2D6). The sensitivity of human and dog spheroids is compared after a 48h single exposure (**E**) and 7 days repeated exposures (**F**) for acetaminophen (APAP), troglitazone (TRO), and chlorpromazine (CPZ). Three concentrations (1x, 5x, and 20x c_{max}) are tested per compound. Error bars indicate SEM. *, **, and *** correspond to $p < 0.05$, $p < 0.01$, and $p < 0.001$ in two-tailed heteroscedastic t-tests, respectively.

tained high viability except for spheroids generated in PE96 plates in which 20x c_{max} concentration was clearly toxic. Across plates, spheroid sensitivity to TRO and CPZ was similar, with one exception. While TRO showed toxicity only after repeated exposure with the highest concentration in all plates, this drug was clearly hepatotoxic already at 5x Cmax for spheroids generated in Biofloat96 plate. Compared to PHH spheroids, PCH aggregates were overall less sensitive to all compounds tested, particularly after repeated exposure.

To the best of our knowledge, these results constitute the first demonstration that primary canine hepatocyte aggregates can be stably cultured for multiple weeks. Culture in chemically defined serum-free media with identical compositions as for PHH spheroids facilitates the overall maintenance of molecular phenotypes and functions and is compatible with both acute and chronic toxicity tests, thus establishing these three-dimensional aggregates as a viable model for translational applications. However, the choice of microplate is of tremendous importance to enable successful formation of PCH three-dimensional culture models.

4 | DISCUSSION

Protocol standardization is imperative to facilitate the acceptance of three-dimensional tissue models as reliable preclinical assays. As of September 2023, more than 4500 spheroid experiments can be retrieved from the MISpheroID database, indicating that the potential of the spheroid model in biomedical research is increasingly recognized [35]. Notably, comparison of the different selected spheroid methods revealed diverse impacts on spheroid metrics, thus indicating the need for careful benchmarking. For liver spheroids, this should encompass the choice of cell model, seeding protocol, media composition as well as microplates. Most of these parameters have been benchmarked in recent studies. The phenotype and function of primary hepatocytes have been shown to be superior to hepatoma cells and stem cell-derived hepatocytes [36–39]. Furthermore, the effects of different spheroid formation protocols and media compositions have been extensively evaluated. Our study is the first to test the impacts of different microplates and demonstrates that they can have pronounced impacts on formation kinetics, morphology, gene expression patterns, compound toxicity and long-term stability. While effects on human liver spheroids were mostly quantitative, strong qualitative differences were observed for canine hepatocyte spheroids, which could only be successfully formed in six out of the ten plates tested.

To implement three-dimensional liver spheroids in preclinical pharmacology and toxicology, reproducibility of spheroid formation plays a crucial role. This in turn requires that all seeded cells integrate into one structure and form a single spheroid in each well. The formation of one spheroid per well could be achieved in all tested plates, except for Greiner384 plates in which cell aggregation resulted in multiple spheroids per well. In addition to reproducibility, rapid spheroid formation is important, particularly in the context of using three-dimensional liver spheroids for drug screening and toxicological analyses. Compaction of PHH seeded in Biofloat384 was the fastest among the investigated plates, resulting in spheroid formation already at 3 days after cell seeding while 5 to 6 days were required in all other tested plates. Interestingly, PCH aggregated more loosely compared to PHH across all microplates. As a result, aggregation was slower (10 days vs. 7 days) and only 6 out of 10 microplates supported the formation of PCH aggregates.

Cultivation of three-dimensional liver spheroids for multiple weeks is essential for chronic disease modelling and repeated drug exposures. Our data indicate that Corning and Biofloat microplates, both in 96- and 384-well formats, are best suited for long-term culture. Which factors are driving these differences however, remains unclear. Previous studies demonstrated that E-cadherin-mediated cell-cell interactions inhibit apoptosis and promote cell survival in human liver spheroids compared to isolated cells or two-dimensional cultures [40]. Further factors with potential impacts on cell viability include microstructure and leaching of compounds from the coating itself or the underlying bulk material [41–43].

In addition to changes in long-term viability, we also observed that the choice of microplate affected gene expression patterns. We have previously reported that primary hepatocytes undergo dynamic transcriptomic changes during aggregation into spheroids which recapitulate molecular events observed during liver regeneration [44]. Based on these findings, one can assume that differences in aggregation kinetics between plates could directly translate into altered expression patterns. These findings have important implications as they suggest that the use of different plates could have significant impacts on the biological interpretations of the obtained results even if otherwise identical protocols are used.

Different microplates furthermore affected the sensitivity of liver spheroids to hepatotoxins with different modes of action. APAP hepatotoxicity is caused by its metabolic byproduct, the reactive metabolite N-acetyl-p-benzoquinonimine (NAPQI). As NAPQI formation is dependent on the hepatic enzymes CYP2E1 and CYP3A4, dedifferentiated and metabolically inactive hepatic cell models are largely protected from APAP toxicity [45]. Here we find that APAP sensitivity of PHH spheroids was overall similar across plates, which is in agreement with similar expression levels of CYP2E1 and CYP3A4. In contrast, CPZ and TRO exert toxicity at least in part by inhibiting the bile salt export pump (BSEP; encoded by *ABCB11*) at the transcriptional and/or protein level [46,47]. At high concentrations, both compounds were clearly toxic across all microplates; however, toxicity of these compounds at lower concentrations (CPZ 1x c_{max} and TRO 5x c_{max}) differed by > 10-fold, with spheroids cultivated in Nunc96 plates being the most resistant. These results align with increased BSEP expression in this plate type, which might bestow hepatocytes with an increased capacity to export bile salts and thus blunt CPZ and TRO toxicity. Differences in the sensitivity to hydrophobic compounds between different plates may be also due to differences in compound absorption. Cell culture plastics are prone to absorption of hydrophobic small molecules [48]. TRO and CPZ are both hydrophobic with *logP* values of 3.6 and 5.18, respectively, whereas APAP is hydrophilic (*logP* = 0.51). Different surface treatments may reduce absorption, resulting in different free concentrations, which translates into altered compound sensitivity at

the same nominal exposure concentration. Minimizing drug absorption thus provides an important direction for the optimization of ULA coating strategies.

In summary, by comparing morphology, phenotype and function of isogenic liver spheroids in side-by-side experiments, we demonstrated diverse impacts of the choice of ULA microplates. While most plates supported the formation of human liver spheroids, large plate differences were observed in hepatic gene expression and toxicity assays. Overall, spheroids in Corning and Biofloat plates exhibited the highest viability, metabolic activity and sensitivity to hepatotoxins. Thus, our results suggest that these plates are suitable for the generation of human liver models that can be implemented in preclinical drug development. However, liver spheroids cultivated in these plates still showed assay-specific differences and it is thus recommended that researchers evaluate the suitability of these plates for their own experiments and purposes. We furthermore provide the first characterization of three-dimensional spheroids from primary hepatocytes of Beagle dogs and demonstrate their compatibility with long-term pharmacological and toxicological studies. Combined, our results demonstrate how different microplates can affect results of spheroid assays and provide useful information for the optimization of future liver spheroid experiments.

AUTHOR CONTRIBUTIONS

Conceptualization: Chen Xing, Aurino Kemas, Volker M. Lauschke; Formal analysis: Chen Xing, Aurino Kemas, Kathrin Klein; Funding acquisition: Per Artursson, Volker M. Lauschke; Investigation: Chen Xing, Aurino Kemas, Evgeniya Mickols, Kathrin Klein; Project administration: Volker M. Lauschke; Resources: Per Artursson, Volker M. Lauschke; Supervision: Aurino Kemas, Volker M. Lauschke; Visualization: Chen Xing, Volker M. Lauschke; Writing – original draft: Chen Xing; Writing – review & editing: Aurino Kemas, Volker M. Lauschke.

ACKNOWLEDGMENTS

The project was financed by faCellitate GmbH. The study sponsor was involved in experimental planning but did not influence the interpretation of the results. In addition, the authors received support from the Swedish Research Council [grant numbers:2019-01837 2021-02801 and 2023-03015], the Ruth och Richard Julins Foundation for Gastroenterology [grant number 2021-00158] and Robert Bosch Foundation, Stuttgart, Germany. The authors are grateful to Igor Liebermann (IKP Stuttgart) for conducting expression analyses.

CONFLICT OF INTEREST STATEMENT

VML is co-founder, CEO and shareholder of HepaPredict AB, as well as co-founder and shareholder of PersoMedix AB.

DATA AVAILABILITY STATEMENT

The data that support the findings of this study are available from the corresponding author upon reasonable request

ORCID

Volker M. Lauschke https://orcid.org/0000-0002-1140-6204

REFERENCES

1. Weaver, R. J., Blomme, E. A., Chadwick, A. E., Copple, I. M., Gerets, H. H. J., Goldring, C. E., Guillouzo, A., Hewitt, P. G., Ingelman-Sundberg, M., Jensen, K. G., Juhila, S., Klingmüller, U., Labbe, G., Liguori, M. J., Lovatt, C. A., Morgan, P., Naisbitt, D. J., Pieters, R. H. H., Snoeys, J., & Park, B. K. (2020). Managing the challenge of drug-induced liver injury: A roadmap for the development and deployment of preclinical predictive models. *Nature Reviews Drug Discovery*, *19*, 131–148.
2. Taylor, K., & Alvarez, L. R. (2019). An estimate of the number of animals used for scientific purposes worldwide in 2015. *Alternatives to Laboratory Animals*, *47*, 196–213.
3. Son, Y.-W., Choi, H.-N., Che, J.-H., Kang, B.-C., & Yun, J.-W. (2020). Advances in selecting appropriate non-rodent species for regulatory toxicology research: Policy, ethical, and experimental considerations. *Regulatory Toxicology and Pharmacology*, *116*, 104757.
4. Hackam, D. G., & Redelmeier, D. A. (2006). Translation of research evidence from animals to humans. *Journal of the American Medical Association*, *296*, 1731–1732.
5. Perel, P., Roberts, I., Sena, E., Wheble, P., Briscoe, C., Sandercock, P., Macleod, M., Mignini, L. E., Jayaram, P., & Khan, K. S. (2007). Comparison of treatment effects between animal experiments and clinical trials: Systematic review. *Bmj*, *334*, 197.
6. Bailey, J., Thew, M., & Balls, M. (2015). Predicting human drug toxicity and safety via animal tests: Can any one species predict drug toxicity in any other, and do monkeys help? *Alternatives to Laboratory Animals*, *43*, 393–403.
7. Turner, J., Pound, P., Owen, C., Hutchinson, I., Hop, M., Chau, D. Y. S., Silva, L. V. B., Coleman, M., Dubourg, A., Harries, L. W., Hutter, V., Kenna, J. G., Lauschke, V. M., Neuhaus, W., Roper, C., Watkins, P. B., Welch, J., Alvarez, L. R., & Taylor, K. (2022). Incorporating new approach methodologies into regulatory nonclinical pharmaceutical safety assessment. *Altex*, *40*, 519–533.
8. Han, J. J. (2023). FDA Modernization Act 2.0 allows for alternatives to animal testing. *Artificial Organs*, *47*, 449–450.
9. Underhill, G. H., & Khetani, S. R. (2018). Bioengineered liver models for drug testing and cell differentiation studies. *Cellular and Molecular Gastroenterology and Hepatology*, *5*, 426–439.
10. Lauschke, V. M., Zandi Shafagh, R., Hendriks, D. F. G., & Ingelman-Sundberg, M. (2019). 3D primary hepatocyte culture systems for analyses of liver diseases, drug metabolism, and toxicity: Emerging culture paradigms and applications. *Biotechnology Journal*, *14*, e1800347.
11. Yadav, J., Hassani, M. E., Sodhi, J., Lauschke, V. M., Hartman, J. H., & Russell, L. E. (2021). Recent developments in in vitro and in vivo models for improved translation of preclinical pharmacokinetics and pharmacodynamics data. *Drug Metabolism Reviews*, *53*, 207–233.
12. Yang, S., Ooka, M., Margolis, R. J., & Xia, M. (2023). Liver three-dimensional cellular models for high-throughput chemical testing. *Cell Reports Methods*, *3*, 100432.
13. Bell, C. C., Lauschke, V. M., Vorrink, S. U., Palmgren, H., Duffin, R., Andersson, T. B., & Ingelman-Sundberg, M. (2017). Transcriptional, functional, and mechanistic comparisons of stem cell–derived hepatocytes, HepaRG cells, and three-dimensional human hepatocyte spheroids as predictive in vitro systems for drug-induced liver injury. *Drug Metabolism and Disposition*, *45*, 419–429.
14. Vorrink, S. U., Ullah, S., Schmidt, S., Nandania, J., Velagapudi, V., Beck, O., Ingelman-Sundberg, M., & Lauschke, V. M. (2017). Endogenous and xenobiotic metabolic stability of primary human hepatocytes in long-term 3D spheroid cultures revealed by a combination of targeted and untargeted metabolomics. *FASEB Journal*, *31*, 2696–2708.
15. Messner, S., Fredriksson, L., Lauschke, V. M., Roessger, K., Escher, C., Bober, M., Kelm, J. M., Ingelman-Sundberg, M., & Moritz, W. (2018). Transcriptomic, proteomic, and functional long-term characterization of multicellular three-dimensional human liver microtissues. *Applied In Vitro Toxicology*, *4*, 1–12.

16. Vorrink, S. U., Zhou, Y., Ingelman-Sundberg, M., & Lauschke, V. M. (2018). Prediction of drug-induced hepatotoxicity using long-term stable primary hepatic 3D spheroid cultures in chemically defined conditions. *Toxicological Sciences*, *163*, 655–665.
17. Proctor, W. R., Foster, A. J., Vogt, J., Summers, C., Middleton, B., Pilling, M. A., Shienson, D., Kijanska, M., Ströbel, S., Kelm, J. M., Morgan, P., Messner, S., & Williams, D. (2017). Utility of spherical human liver microtissues for prediction of clinical drug-induced liver injury. *Archives of Toxicology*, *91*, 2849–2863.
18. Riede, J., Wollmann, B. M., Molden, E., & Ingelman-Sundberg, M. (2021). Primary human hepatocyte spheroids as an in vitro tool for investigating drug compounds with low hepatic clearance. *Drug Metabolism and Disposition*, *49*, 501–508.
19. Kanebratt, K. P., Janefeldt, A., Vilén, L., Vildhede, A., Samuelsson, K., Milton, L., Björkbom, A., Persson, M., Leandersson, C., Andersson, T. B., & Hilgendorf, C. (2021). Primary human hepatocyte spheroid model as a 3D in vitro platform for metabolism studies. *Journal of Pharmaceutical Sciences*, *110*, 422–431.
20. Preiss, L. C., Lauschke, V. M., Georgi, K., & Petersson, C. (2022). Multi-well array culture of primary human hepatocyte spheroids for clearance extrapolation of slowly metabolized compounds. *The Aaps Journal [Electronic Resource]*, *24*, 41.
21. Sakalem, M. E., de Sibio, M. T., da Silva da Costa, F. A., & de Oliveira, M. (2021). Historical evolution of spheroids and organoids, and possibilities of use in life sciences and medicine. *Biotechnology Journal*, *16*, e2000463.
22. Ingelman-Sundberg, M., & Lauschke, V. M. (2021). 3D human liver spheroids for translational pharmacology and toxicology. *Basic & Clinical Pharmacology & Toxicology*, *130*(1), 5–15.
23. Handin, N., Mickols, E., Ölander, M., Rudfeldt, J., Blom, K., Nyberg, F., Senkowski, W., Urdzik, J., Maturi, V., Fryknäs, M., & Artursson, P. (2021). Conditions for maintenance of hepatocyte differentiation and function in 3D cultures. *Iscience*, *24*, 103235.
24. Costa, E. C., de Melo-Diogo, D., Moreira, A. F., Carvalho, M. P., & Correia, I. J. (2018). Spheroids formation on non-adhesive surfaces by liquid overlay technique: Considerations and practical approaches. *Biotechnology Journal*, *13*, 1.
25. Nakazawa, K., Izumi, Y., & Mori, R. (2009). Morphological and functional studies of rat hepatocytes on a hydrophobic or hydrophilic polydimethylsiloxane surface. *Acta Biomaterialia*, *5*, 613–620.
26. Chou, S.-F., Lai, J.-Y., Cho, C.-H., & Lee, C.-H. (2016). Relationships between surface roughness/stiffness of chitosan coatings and fabrication of corneal keratocyte spheroids: Effect of degree of deacetylation. *Colloids and Surfaces. B, Biointerfaces*, *142*, 105–113.
27. Tsai, Y. A., Li, T., Torres-Fernández, L. A., Weise, S. C., Kolanus, W., & Takeoka, S. (2021). Ultra-thin porous PDLLA films promote generation, maintenance, and viability of stem cell spheroids. *Frontiers in Bioengineering and Biotechnology*, *9*, 674384.
28. Palmgrén, J. J., Mönkkönen, J., Korjamo, T., Hassinen, A., & Auriola, S. (2006). Drug adsorption to plastic containers and retention of drugs in cultured cells under in vitro conditions. *European Journal of Pharmaceutics and Biopharmaceutics*, *64*, 369–378.
29. Ölander, M., Wegler, C., Flörkemeier, I., Treyer, A., Handin, N., Pedersen, J. M., Vildhede, A., Mateus, A., LeCluyse, E. L., Urdzik, J., & Artursson, P. (2021). Hepatocyte size fractionation allows dissection of human liver zonation. *Journal of Cellular Physiology*, *236*, 5885–5894.
30. Bell, C. C., Hendriks, D. F. G., Moro, S. M. L., Ellis, E., Walsh, J., Renblom, A., Puigvert, L. F., Dankers, A. C. A., Jacobs, F., Snoeys, J., Sison-Young, R. L., Jenkins, R. E., Nordling, Å., Mkrtchian, S., Park, B. K., Kitteringham, N. R., Goldring, C. E. P., Lauschke, V. M., & Ingelman-Sundberg, M. (2016). Characterization of primary human hepatocyte spheroids as a model system for drug-induced liver injury, liver function and disease. *Scientific Reports*, *6*, 25187.
31. Lin, R.-Z., Chou, L.-F., Chien, C.-C. M., & Chang, H.-Y. (2006). Dynamic analysis of hepatoma spheroid formation: Roles of E-cadherin and β1-integrin. *Cell and Tissue Research*, *324*, 411–422.
32. Chua, A. C. Y., Ananthanarayanan, A., Ong, J. J. Y., Wong, J. Y., Yip, A., Singh, N. H., Qu, Y., Dembele, L., McMillian, M., Ubalee, R., Davidson, S., Tungtaeng, A., Imerbsin, R., Gupta, K., Andolina, C., Lee, F., Tan, K. S.-W., Nosten, F., Russell, B., & Bifani, P. (2019). Hepatic spheroids used as an in vitro model to study malaria relapse. *Biomaterials*, *216*, 119221.
33. Kyffin, J. A., Sharma, P., Leedale, J., Colley, H. E., Murdoch, C., Harding, A. L., Mistry, P., & Webb, S. D. (2019). Characterisation of a functional rat hepatocyte spheroid model. *Toxicology in Vitro*, *55*, 160–172.
34. Nautiyal, M., Qasem, R. J., Fallon, J. K., Wolf, K. K., Liu, J., Dixon, D., Smith, P. C., & Mosedale, M. (2021). Characterization of primary mouse hepatocyte spheroids as a model system to support investigations of drug-induced liver injury. *Toxicology in Vitro*, *70*, 105010.
35. Peirsman, A., Blondeel, E., Ahmed, T., Anckaert, J., Audenaert, D., Boterberg, T., Buzas, K., Carragher, N., Castellani, G., Castro, F., Dangles-Marie, V., Dawson, J., Tullio, P. D., Vlieghere, E. D., Dedeyne, S., Depypere, H., Diosdi, A., Dmitriev, R. I., Dolznig, H., & Wever, O. D. (2021). MISpheroID: A knowledgebase and transparency tool for minimum information in spheroid identity. *Nature Methods*, *18*, 1294–1303.
36. Wilkening, S., Stahl, F., & Bader, A. (2003). Comparison of primary human hepatocytes and hepatoma cell line Hepg2 with regard to their biotransformation properties. *Drug Metabolism and Disposition*, *31*, 1035–1042.
37. Berger, B., Donzelli, M., Maseneni, S., Boess, F., Roth, A., Krähenbühl, S., & Haschke, M. (2016). Comparison of liver cell models using the basel phenotyping cocktail. *Frontiers in Pharmacology*, *7*, 443.
38. Sison-Young, R. L., Lauschke, V. M., Johann, E., Alexandre, E., Anthérieu, S., Aerts, H., Gerets, H. H. J., Labbe, G., Hoët, D., Dorau, M., Schofield, C. A., Lovatt, C. A., Holder, J. C., Stahl, S. H., Richert, L., Kitteringham, N. R., Jones, R. P., Elmasry, M., Weaver, R. J., & Park, B. K. (2017). A multicenter assessment of single-cell models aligned to standard measures of cell health for prediction of acute hepatotoxicity. *Archives of Toxicology*, *91*, 1385–1400.
39. Huggett, Z. J., Smith, A., Vivo, N. D., Gomez, D., Jethwa, P., Brameld, J. M., Bennett, A., & Salter, A. M. (2022). A comparison of primary human hepatocytes and hepatoma cell lines to model the effects of fatty acids, fructose and glucose on liver cell lipid accumulation. *Nutrients*, *15*, 40.
40. Luebke-Wheeler, J. L., Nedredal, G., Yee, L., Amiot, B. P., & Nyberg, S. L. (2009). E-cadherin protects primary hepatocyte spheroids from cell death by a caspase-independent mechanism. *Cell Transplantation*, *18*, 1281–1287.
41. Bartolo, L. D., Catapano, G., Volpe, C. D., & Drioli, E. (1999). The effect of surface roughness of microporous membranes on the kinetics of oxygen consumption and ammonia elimination by adherent hepatocytes. *Journal of Biomaterials Science Polymer Edition*, *10*, 641–655.
42. Krasteva, N., Groth, Th., Fey-Lamprecht, F., & Altankov, G. (2001). The role of surface wettability on hepatocyte adhesive interactions and function. *Journal of Biomaterials Science Polymer Edition*, *12*, 613–627.
43. Palaniappan, S., Sadacharan, C. M., & Rostama, B. (2022). Polystyrene and polyethylene microplastics decrease cell viability and dysregulate inflammatory and oxidative stress markers of MDCK and L929 cells in vitro. *Exposure and Health*, *14*, 75–85.
44. Oliva-Vilarnau, N., Vorrink, S. U., Ingelman-Sundberg, M., & Lauschke, V. M. (2020). A 3D cell culture model identifies Wnt/ β -catenin mediated inhibition of p53 as a critical step during human hepatocyte regeneration. *Advancement of Science*, *7*, 2000248.

45. Zhou, Y., Shen, J. X., & Lauschke, V. M. (2019). Comprehensive evaluation of organotypic and microphysiological liver models for prediction of drug-induced liver injury. *Frontiers in Pharmacology*, *10*, 1093.
46. Dawson, S., Stahl, S., Paul, N., Barber, J., & Kenna, J. G. (2012). In vitro inhibition of the bile salt export pump correlates with risk of cholestatic drug-induced liver injury in humans. *Drug Metabolism and Disposition*, *40*, 130–138.
47. Pedersen, J. M., Matsson, P., Bergström, C. A. S., Hoogstraate, J., Norén, A., LeCluyse, E. L., & Artursson, P. (2013). Early identification of clinically relevant drug interactions with the human bile salt export pump (BSEP/ABCB11). *Toxicological Sciences*, *136*, 328–343.
48. Kemas, A. M., Zandi Shafagh, R., Taebnia, N., Michel, M., Preiss, L., Hofmann, U., & Lauschke, V. M. (2023). Compound absorption in polymer devices impairs the translatability of preclinical safety assessments. *Advanced Healthcare Materials*, e2303561.

SUPPORTING INFORMATION

Additional supporting information can be found online in the Supporting Information section at the end of this article.

How to cite this article: Xing, C., Kemas, A., Mickols, E., Klein, K., Artursson, P., & Lauschke, V. M. (2024). The choice of ultra-low attachment plates impacts primary human and primary canine hepatocyte spheroid formation, phenotypes, and function. *Biotechnology Journal*, *19*, e2300587. https://doi.org/10.1002/biot.202300587